

Three-Dimensional Evaluation of the Accuracy of Zygomatic Implant Placement Through an In-House Fully Guided Approach

Federico Hernández-Alfaro, MD, DDS, PhD^{1,2}/Jorge Bertos-Quílez, DDS, MSc, PhD¹/
Adaia Valls-Ontañón, MD, DDS, PhD^{1,2}/Daniel Paternostro-Betancourt, DDS, MSc¹/
Foskolos Pindaros-Georgios, DDS, MSc¹/Gian Maria Ragucci, DDS, MSc¹

Purpose: To validate guided surgery for zygomatic implants (ZIs) by analyzing the final position of the implants relative to the preoperatively planned position. **Material and Methods:** Five patients with fully edentulous atrophic maxillae treated with four ZIs through a fully guided implant surgical approach were evaluated. The preoperative phase included digital planning, through which the surgical guide was designed and created. Analysis of the guided surgery accuracy was carried out by superimposing the digital planning over the final position of the implants using preoperative and post-operative CBCT. The radiologic evaluation included implant angular deviation, entrance deviation, exit deviation, platform deviation, and apex apicocoronal and mesiodistal deviation. **Results:** All five patients (two men and three women; mean age: 61.8 ± 3 years) were each treated with four ZIs using a fully guided approach with an extrasinusal path, obtaining ideal emergence of the implants. Superimposition comparison found a mean axial angular implant deviation of 0.79 ± 0.41 degrees and a mean implant entrance deviation of 0.95 ± 0.26 degrees. The platform deviation was 0.62 ± 0.19 mm buccopalatally and 0.76 ± 0.14 mm mesiodistally, while the apical deviation was 0.42 ± 0.13 mm buccopalatally and 1.06 ± 0.37 mm mesiodistally. **Conclusions:** Guided surgery in zygomatic implants appears to be sufficiently accurate to make it a safe and predictable technique. *Int J Oral Maxillofac Implants* 2023;38:747–756. doi: 10.11607/jomi.10045

Keywords: computer-guided surgery, oral and maxillofacial, zygomatic implants

Progressive bone loss caused by dental extraction and maxillary sinus pneumatization can lead to advanced degrees of maxillary alveolar bone atrophy, such as classes V and VI from the Cawood and Howell classification.¹ In highly reabsorbed maxillary alveolar ridges, the placement of implants in anatomical buttresses is considered an alternative to bone reconstructive procedures.^{2–5} However, due to the remote position of such structures, especially the zygomatic buttress, access is complicated and the correct execution of the implant placement is dependent upon the experience of the surgeon. Nowadays, sophisticated planning software and diagnostic imaging techniques are becoming more precise, allowing researchers to study and simulate the execution of surgical procedures, as well as to transfer the simulation accurately into practice using

computer-guided surgery.^{6,7} In this regard, implant placement using computer-guided techniques results in shorter surgery times, less discomfort for the patient, and more precise implant placement than freehand implant surgery, especially in the aforementioned blind procedures.^{8–10}

To allow for the ideal placement of zygomatic implants (ZIs) in the malar bone and enhance prosthetic emergence after virtual 3D planning, two methods have been described in the literature: customized surgical guides or computer-aided surgical navigation systems.^{11–13} Computer-aided surgical navigation offers constant intraoperative visualization of the tip of the drilling bur. This enables the surgeon to precisely guide the drill to control the implant axis and ensure optimum bone anchorage.¹⁴ However, on-site navigation is expensive and prolongs the operation time, though it also theoretically guarantees exact placement of the implant and optimal bone anchorage. In practice, though, this tool is not exempt from error.¹⁵

Guided surgery with ZIs has been studied on stereolithographic models and cadavers, with good results.^{13,16,17} However, some authors have demonstrated that the use of surgical customized drilling guides in the context of ZI placement on stereolithographic models should be reevaluated, because some major deviations have been noted.^{18,19}

¹Department of Oral and Maxillofacial Surgery, Universitat Internacional de Catalunya, Barcelona, Spain.

²Institute of Maxillofacial Surgery, Teknon Medical Center, Barcelona, Spain.

Correspondence to: Gian Maria Ragucci, DDS, Department of Oral and Maxillofacial Surgery, Universitat Internacional de Catalunya Josep Trueta, s/n 08195 - Sant Cugat del Vallès, Barcelona, Spain. Email: gian1@uic.es

Submitted May 5, 2022; accepted February 3, 2023.

©2023 by Quintessence Publishing Co Inc.

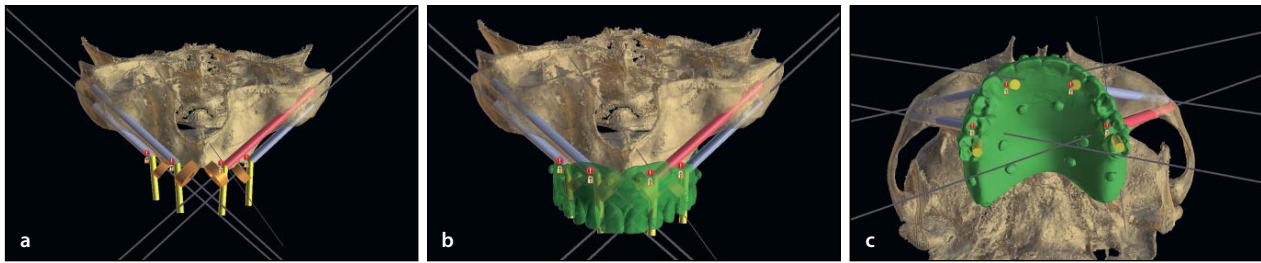


Fig 1 (a) Frontal view of the preoperative zygomatic implant planification. (b) Preoperative zygomatic implant planification with the STL of the prosthesis superimposed from the frontal and (c) crestal view.

To the present authors' knowledge, no in vivo studies to date have evaluated the accuracy of surgical guides for ZI placement. Therefore, the main objective of the present study was to evaluate the accuracy of guided surgery in the context of ZI placement by analyzing the final 3D position of the implants relative to the preoperatively planned position with the purpose of validating this technique.

MATERIAL AND METHODS

Study Design

Five consecutive patients with fully edentulous atrophic maxillae (Cawood and Howell class VI) were evaluated.¹ All patients were treated with four ZIs using a fully guided surgery approach at the Department of Oral and Maxillofacial Surgery of the Universitat Internacional de Catalunya between September 2020 and December 2021. The study was approved by the local Ethics Committee (CIR-ECL 2021-01).

Patient Selection

The inclusion criteria were as follows: patients who had a fully edentulous maxilla in which treatment with conventional implants or without using bone grafting, Le Fort I osteotomy, or distraction osteogenesis procedures was ruled out. Moreover, good systemic health [ASA (American Society of Anesthesiologists) score I to II] was required, along with patient commitment to attend all the study visits. Patients were excluded if they presented a medical history contraindicating surgery; any disease, condition, or medication that might compromise soft and hard tissue healing, such as chemotherapy or head and neck radiotherapy in the previous 5 years; toxic habits capable of compromising recovery and bone healing; active sinus disorders; or the presence of sufficient maxillary bone to allow rehabilitation using conventional implants.

The study was conducted in accordance with the ethical standards laid down in the Declaration of Helsinki (1964 and subsequent amendments). All participants signed an informed consent agreement prior to surgery.

Digital Planning

Initially, the new dentures provided stable occlusion and function to all patients according to the appropriate prosthetic and occlusal parameters. Composite markers were placed on the vestibular and palatal sides of the maxillary dentures, and then the denture was scanned with a 3Shape TRIOS scanner.

A CBCT image was obtained with the i-CAT Cone Beam 3D Imaging device (i-CAT FLX V-Series, DEXIS) with a setting of 120 kVp, 10.11 mA, voxel size 0.4 mm, and a field of view of 13 × 17 cm. While performing the CBCT scans, the dentures with the markers were placed in the correct position. Zygomatic implant planning was carried out with Blue Sky Plan software version 4.7.20 (Blue Sky Bio). The STL (standard tessellation language) file of the denture was superimposed with the DICOM file by using the balls of composite as reference points. Thus, the ideal relationship between the bone structure and the prosthetic design could be visualized on the software. The ZI implants were virtually positioned following maximum bone anchorage and the ideal implant prosthetic emergence profiles and bone thickness availability^{20,21} (Fig 1).

The digital design of the surgical guide began with segmentation of the maxillary bone. The segmentation of the maxilla DICOM file was performed with the "Segmentation" panel of the "Model Edition" module of the Blue Sky Plan software. In accordance with the visual evaluation of the digital designer, the osseous areas were marked in the apicocoronal and sagittal directions on all layers using the "Brush" tool. The segmentation allowed the DICOM file to be turned into an STL file that provided the software with a physical surface for the fabrication of the surgical guide. Once the segmentation was completed, the alveolar position of the ZI was prosthetically driven into the crestal area of the residual ridge following an extrasinusual path with intimate contact to achieve apical anchorage in the zygomatic bone. A safety distance of 5 mm apically from the orbital rim was preserved.

For the osteotomy, two different guides were designed. One was for use only with the 2.35-mm drill (guide A), while the second guide was used for the rest of the drilling sequence, which included the 3.75-mm



Fig 2 Crestal view of the tubes of the two types of guides. The tube of guide A (right tube) provided the metal sleeve on the first 4.5 mm, while the apical portion had a diameter that corresponded to the pilot drill diameter (2.35 ± 0.15 mm). The tube of guide B (left tube) provided only the metal sleeve for the first 4.5 mm crestally, and the rest of the tube interior was free of resin volume.

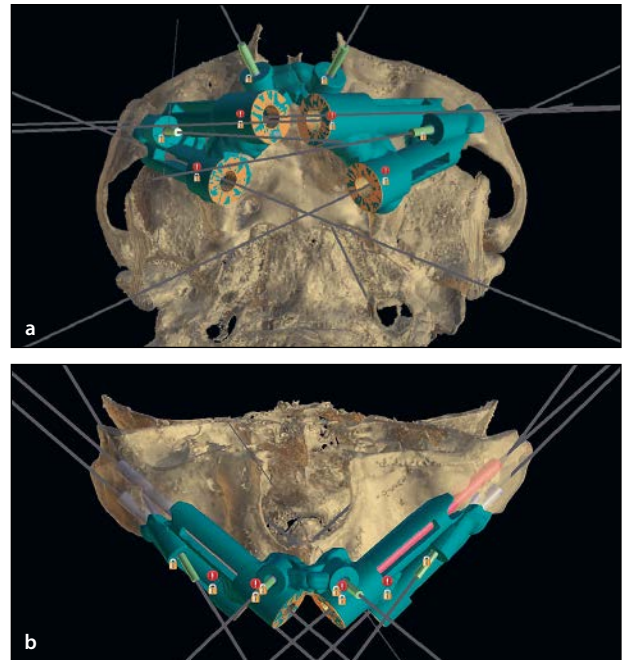


Fig 3 Surgical guide planification. (a) Crestal view of guide A and (b) frontal view of guide B.

drill, the 4.0-mm drill, and the implant placement drill (guide B). The tubes of guide A had a wide enough diameter to allow the insertion of a Neodent metal sleeve ($\varnothing 5.1 \pm 0.15$ mm) along the first 4.5 mm. The diameter of the rest of the tube corresponded to the diameter of the $\varnothing 2.35 \pm 0.15$ mm drill and extended from the apical edge of the metal sleeve to the contact level with the malar bone. However, the tubes of guide B provided only the appropriate crestal diameter to insert a Neodent metal sleeve, while the rest of the structure of the tube was free of any internal resin structure and provided only the support of the whole guide over the malar bone and no guidance of the drills or the implant insertion. The lengths of the tubes were adapted over the anatomy and height of the maxilla of each patient. Finally, four fixation pins were planned to secure the guide: two in the premaxillary area and two in the zygomatic bone (Figs 2 and 3).

The STL files of the surgical guide, the guide tubes, and the segmented maxillary bone were exported from the Blue Sky Plan software and imported into the Autodesk Meshmixer (Autodesk). The final STLs of the surgical guides were printed (Form 2, Formlabs) with biocompatible photopolymer resin (Surgical Guide Resin, Formlabs). After printing, the surgical guides were washed with 70% isopropyl alcohol for 20 minutes using a wash machine (Formlabs), light-cured for 30 minutes at 60°C using the light cure machine (Formlabs),

and sterilized with an autoclave cycle for 15 minutes at 121°C (Line W&H; Fig 4).

Surgical Technique

Implant surgery was performed under conscious sedation and local anesthesia (4% articaine with epinephrine 1:100,000, Normon). A full-thickness mucoperiosteal flap was raised from the maxillary tuberosity of the first quadrant to the contralateral tuberosity of the second quadrant, with two distal releasing incisions and subperiosteal elevation to the floor of the nose in the anterior zone, and to the zygomatic-maxillary buttress and prominence of the zygoma in the lateral zone. Reflection of the palatal flap was done until the alveolar crest width could be properly appraised.

Then, surgical guide A was placed in position and fixed with two fixation pins in the premaxilla, with one fixation pin in the zygoma bone of each maxillary quadrant. Fully guided ZI placement (Zygoma GM, Neodent, Straumann Group) was carried out using the two different guides. The drilling sequence was first performed with the 2.35-mm-diameter drill using guide A, followed by the extraction of guide A and the placement of guide B for the rest of the drilling sequence, which started with the 3.75-mm-diameter drill and concluded with the 4.0-mm-diameter drill. The implants were inserted via the guide tubes.

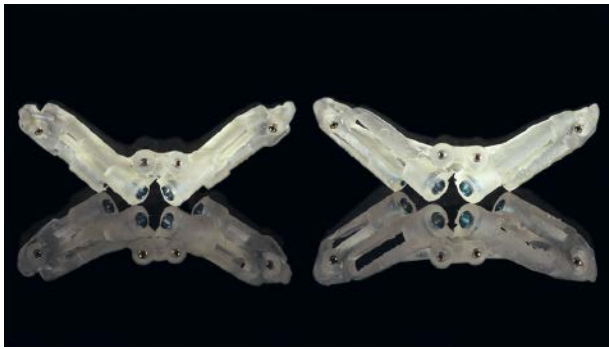


Fig 4 Surgical guide fabrication. Guide A (*left*) was used only for the pilot drill, and guide B (*right*) was used for the subsequent drills and the implant placement.

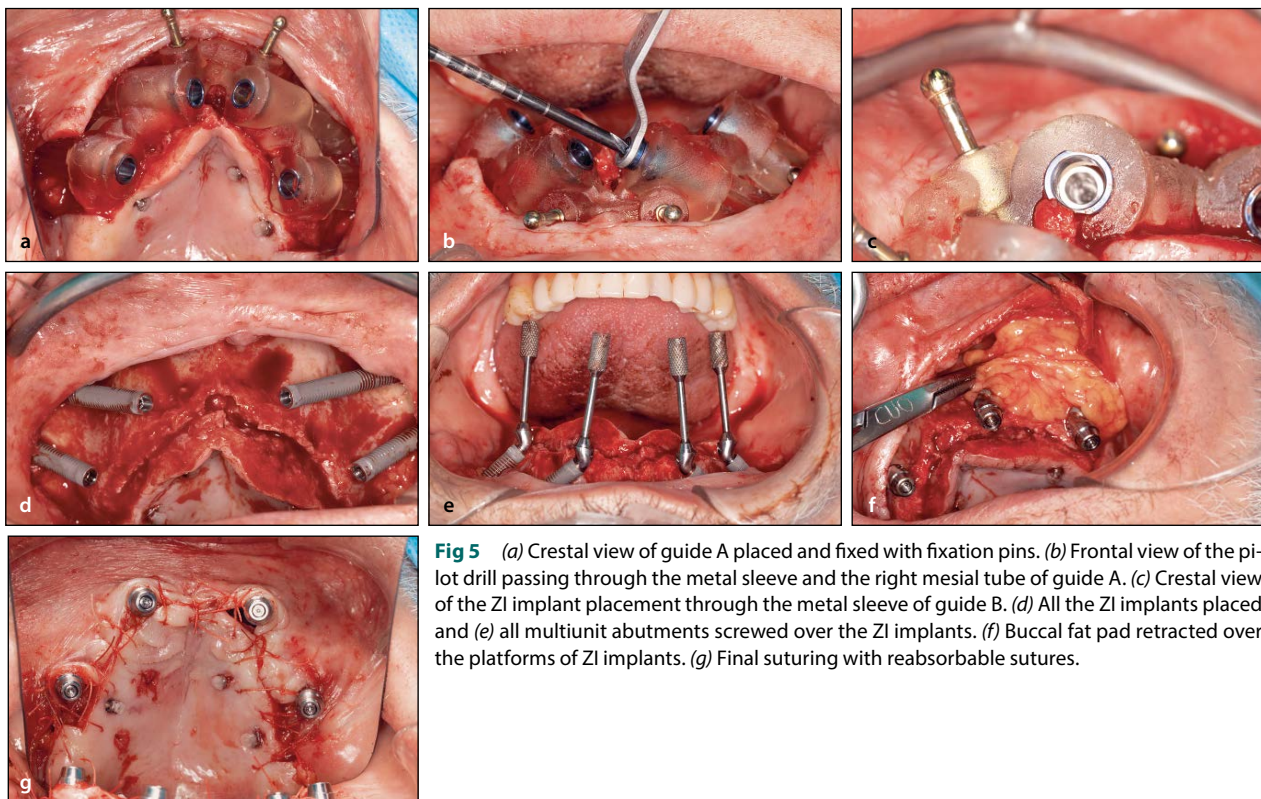


Fig 5 (a) Crestal view of guide A placed and fixed with fixation pins. (b) Frontal view of the pilot drill passing through the metal sleeve and the right mesial tube of guide A. (c) Crestal view of the ZI implant placement through the metal sleeve of guide B. (d) All the ZI implants placed and (e) all multiunit abutments screwed over the ZI implants. (f) Buccal fat pad retracted over the platforms of ZI implants. (g) Final suturing with reabsorbable sutures.

Then, a pedicled buccal fat pad flap was herniated through the vertical releasing incision at the level of the maxillary first molar, adopting a tunnel approach as previously described by Hernández-Alfaro et al.²² The multiunit abutments were connected, allowing the prosthetic screw to access the occlusal aspect of the prosthetic teeth, and the flaps were reapproximated with no tension using interrupted simple sutures (Vicryl 4-0, Ethicon; Fig 5).

An intraoral digital impression was obtained by using the scan bodies over the multiunit abutments and the lower conventional intraoral scan of the mandibular teeth. Then, the scan bodies were replaced with

provisional abutments, and the provisional denture was perforated and attached to the provisional metal abutments using resin while the patient was in maximum intercuspation. A conventional bite registration with bite wax was performed before unscrewing the denture. Using this registration, the technician (F.P.G.) designed and milled the final PMMA fixed provisional prosthesis, which was delivered to the patient 24 hours postsurgery (Fig 6). Patients received antibiotics (875/125 mg amoxicillin/clavulanic acid every 8 hours for 7 days; in case of penicillin allergy, 300 mg clindamycin every 6 hours for 7 days was prescribed), anti-inflammatory and analgesic treatment (prednisone 40 mg once daily



Fig 6 (a to c) Photos of the prosthesis.



Fig 7 Intraoral photo of the immediately loaded prosthesis.

for 4 days; dexketoprofen 25 mg every 8 hours during 7 days; metamizol 575 mg every 8 hours for 7 days), and chlorhexidine rinses (Dentaid, PerioAid 0.20%, twice a day for 2 weeks).

The patients were recalled after 1 week, then again after 1 month. After 3 months of healing, the prosthetic phase was started, and fixed full-arch metal-ceramic prostheses on multiunit abutments were placed (Figs 7 and 8).

Radiological Evaluation

A postoperative CBCT scan was performed after surgery using the i-CAT Cone Beam. The DICOM file of the postoperative maxilla was segmented using Blue Sky Plan software to create an STL file of the postsurgical condition. Afterward, the preoperative segmented maxilla was imported in the Blue Sky Plan software and superimposed with the postoperative STL. The following anatomical structures were used as reference points for superimposition: the infraorbital foramen, the anterior nasal spine, the temporal process of the zygoma bone, and the infraorbital foramen. On the same project, the STL files of the virtual implants of the initial planification were inserted over the preoperative STL

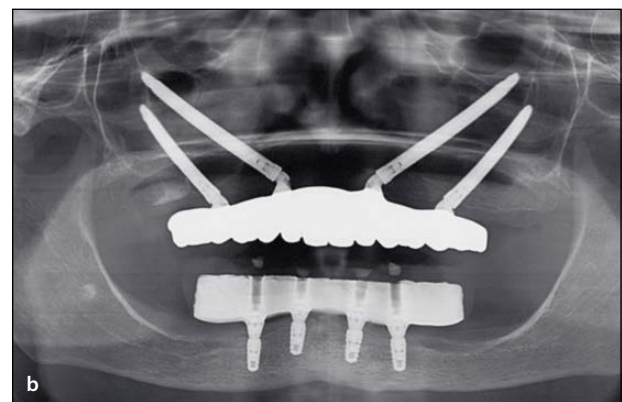
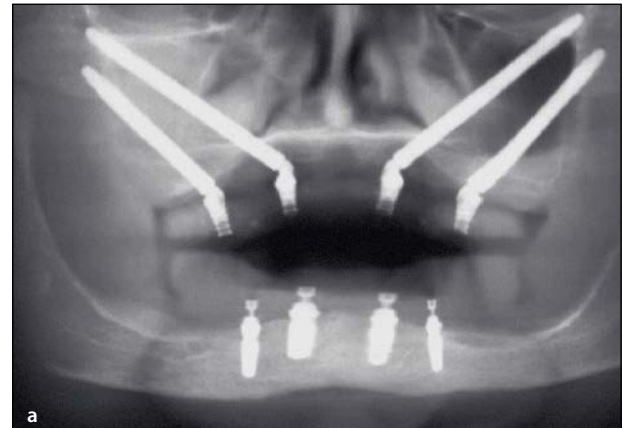


Fig 8 Orthopantomography with (a) provisional prosthesis and (b) final prosthesis delivered.

file with the “Automatic Alignment” option. As a result, the virtual initial implants were superimposed with the real final implant position (Fig 9).

Data Analysis

- Axial angular implant deviation (AID): The angle formed by the axis of the virtual implant crossing the axis of the real implant.
- Implant entrance deviation (IED): The distance between the centers of the platforms of the virtual and real implant.
- Apical mesiodistal deviation (AMDD): The distance between the most mesial point of the virtual implant and most mesial point of the real implant.

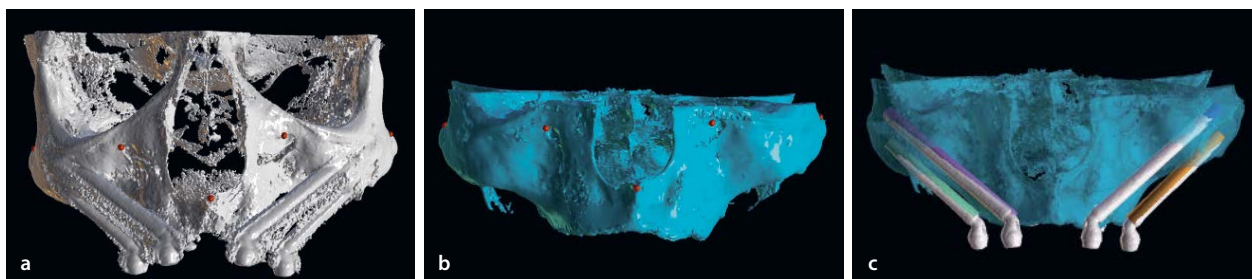


Fig 9 Selection of reference points for the superimposition of the STL file of (a) the segmented postoperative maxilla with the ZI implants placed and (b) the segmented preoperative maxilla. (c) 3D image of the superimposition of the preoperative and postoperative condition.

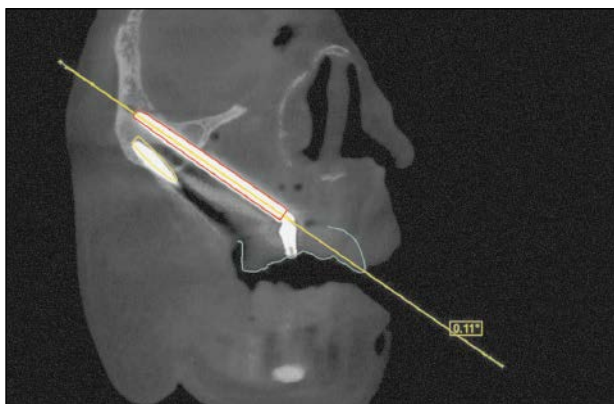


Fig 10 Axial Angular Implant Deviation (AID): In the lateral view, the axis of the virtual and the axis of the real implant were elongated until they contacted each other. The angle between those two lines was measured to find the axial angular deviation.

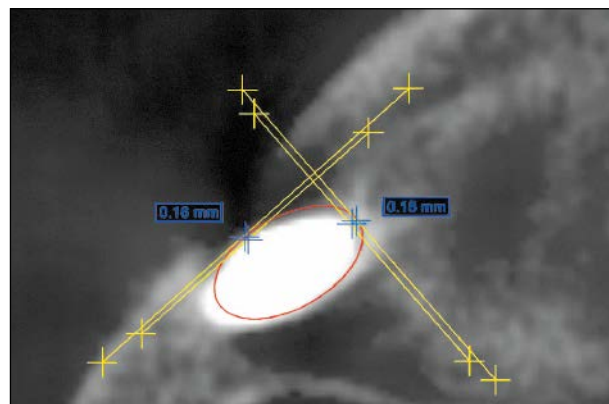


Fig 11 Apical Mesiodistal Deviation (AMDD; right of image): The distance between the most mesial point of the virtual implant (red circle) and most mesial point of the real implant (white circle). Apical Vestibulopalatal Deviation (AVPD; left of image): The distance between the most vestibular point of the virtual implant (red circle) and the most vestibular point of the real implant (white circle).

- Apical vestibulopalatal deviation (AVPD): The distance between the most vestibular point of the virtual implant and the most vestibular point of the real implant.
- Platform buccopalatal deviation (PBPD): The distance between the most vestibular point of the virtual implant and the most vestibular point of the real implant.
- Platform mesiodistal deviation (PMDD): The distance between the most mesial point of the virtual implant and most mesial point of the real implant.
- Implant depth deviation (IDD): The distance between the virtual and real implant depth at platform level.

The deviations were calculated by the digital designer “Distance” and “Angle” tools on Blue Sky Plan software. All registrations were landmark-based. For the angular deviation, the axis of the virtual and the axis of the real implant were elongated in the lateral view until they contacted each other. Then the angle between

those two lines was measured to find the AID. On the same view, the distance from the virtual platform to the real one was calculated with the “Distance” tool to find the IDD. The rest of the measurements were performed on the axial plane with the “Distance” tool. All registrations were landmark based (Figs 10 to 15)

RESULTS

Demographic data and the baseline condition of the five clinical cases are summarized in Table 1. The study sample consisted of two men and three women with a mean age of 61.8 ± 3 years. All five cases were resolved by placing four ZIs using a fully guided approach that employed extrasinusual paths and obtained ideal emergence of the implants. The postoperative courses were uneventful, and no surgical complications such as flap dehiscence, infraorbital nerve damage, involvement of the orbital or infratemporal fossae or intracranial vault, or sinus infections were documented.

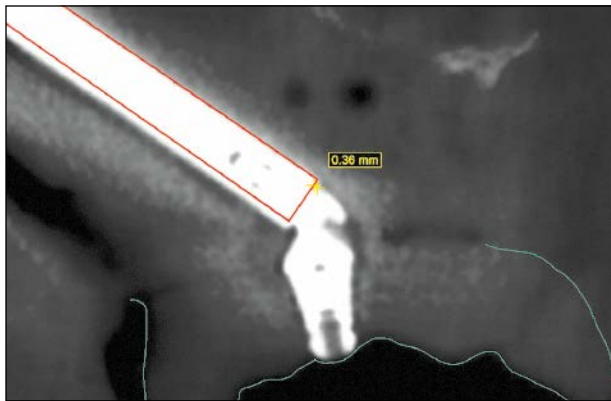


Fig 12 Implant Depth Deviation (IDD): The distance between the virtual and real implant depth at apical and platform level.

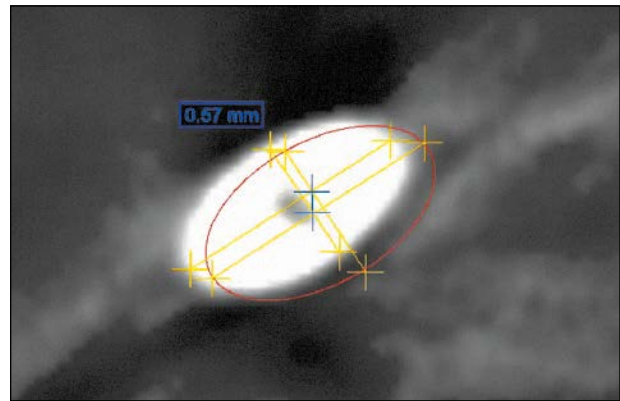


Fig 13 Implant Entrance Deviation (IED): The distance between the center of the virtual implant (red circle) and the center of the real implant (white circle).

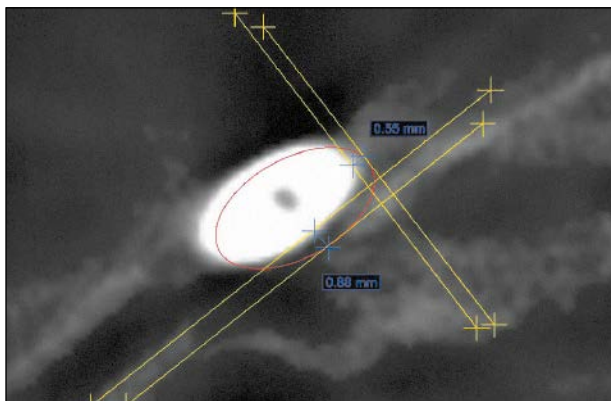


Fig 14 Platform Buccopalatal Deviation (PBPD): The distance between the most vestibular point of the virtual implant (red circle) and the most vestibular point of the real implant (white circle). Platform Mesiodistal Deviation (PMDD): The distance between the most mesial point of the virtual implant (red circle) and most mesial point of the real implant (white circle).

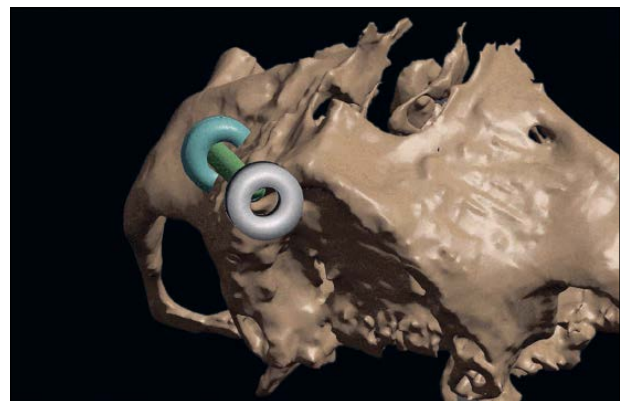


Fig 15 Virtual imaging of a ZI implant (green cylinder) in relation to the crestal sleeve (gray circle) with the corresponding diameter to receive the Neodent metal sleeve of the splint. A copy of the same sleeve (blue circle) is placed more apically along the axis of the ZI implant. The crestal sleeve does not have any conflict with the segmented bone (brown surface) and it can be used. The apical sleeve interferes with the segmented bone, thus it cannot be used due to lack of space for the sleeve and the resin to support the sleeve.

OUTCOME MEASUREMENTS

All ZIs were osseointegrated at 3 months, resulting in a survival rate of 100%. The radiographic outcomes were measured based on the superimposition of the preoperative CBCT scans upon the postoperative scans, resulting in a mean AID between the virtual and real implants of 0.79 ± 0.41 degrees, a mean IED of 0.95 ± 0.26 mm, and a mean IDD of 0.55 ± 0.17 mm.

The results of the radiographic analysis at the level of the implant platform were assessed in the buccopalatal and mesiodistal direction, with mean values of 0.62 ± 0.19 mm and 0.76 ± 0.14 mm, respectively.

Likewise, apical implant deviation was analyzed in the buccopalatal and mesiodistal direction, resulting in mean values of 0.42 ± 0.13 mm and 1.06 ± 0.37 mm, respectively (Table 2).

DISCUSSION

The results of the present study on fully guided ZI placement found the angle of deviation to be 0.79 ± 0.41 degrees, which implies an apical deviation of 0.42 ± 0.13 mm and 1.06 ± 0.37 mm at the buccopalatal and mesiodistal level, respectively. Despite the small sample involved, these results are favorable to validation of the surgical guides for ZI placement. Nevertheless, the authors consider it reasonable to maintain a safe distance from the orbital rim and infra-temporal fossa.

Since the introduction of the quad zygoma protocol in 2004 as a feasible treatment option for cases of advanced maxillary alveolar bone atrophy, it has been well documented in the literature as being a treatment option without any bone grafting related procedures.^{5,14,20}

Table 1 Clinical Case Demographic Data and Baseline Situation

Case	Age (y)	Sex	Smoker	ASA score	Initial situation	ZI position: length
1	58	M	No	I	Fully edentulous	16: 60 mm 13: 52.5 mm 26: 60 mm 23: 45 mm
2	63	F	No	I	Fully edentulous	16: 50 mm 13: 52.5 mm 26: 45 mm 23: 50 mm
3	67	F	No	I	Fully edentulous	16: 60 mm 13: 50 mm 26: 50 mm 23: 45 mm
4	61	M	No	I	Fully edentulous	16: 60 mm 13: 52.5 mm 26: 52.5 mm 23: 45 mm
5	60	F	No	I	Fully edentulous	16: 60 mm 13: 50 mm 26: 52.5 mm 23: 50 mm

M: male; F: female; ZI: zygomatic implant; all implants were Neodent implants (Straumann group). Position refers to FDI tooth position.

In 2006, a new evolution of the technique was introduced that involved exteriorization of the ZI out of the maxillary sinus as a solution to the prosthesis-related issues of the traditional technique.²¹ Since then, no further relevant changes have been made to this technique, though there are well-known risks due to the anatomical zone involved. On the other hand, discouraging results have been published regarding a lack of precision when placing the implants following the previous virtual planning processes.^{18,19} This makes the technique largely dependent upon surgeon expertise, and therefore susceptible to human error.

A virtual 3D planning study found that following extramaxillary zygomatic placement, the average length of ZI housed within the malar bone was 17.42 ± 3.74 mm for anterior implants and 16.48 ± 5.55 mm for posterior implants in the quad zygoma approach.²³ These results corresponded to an in vitro study in which implant planning and placement were performed under optimal conditions. It therefore would be reasonable to focus all efforts on transferring the previously planned ideal 3D implant positioning to clinical practice through safe, precise, and reliable surgical guides. Otherwise, due to the complexity of the placement technique, it would be quite difficult to place the implants in the ideal planned position without a guide.²³

The main concern regarding the use of surgical guides for placing ZIs is the potential discrepancy between the final position of the implant and the virtually planned position. According to the literature, implant placement accuracy is poorer in clinical and cadaver-based studies

than in in vitro studies, especially in terms of horizontal apical deviation and angular deviation.²⁴ A few degrees of difference in the path of the implant can lead to major deviation of the apex, which can result in failures due to the structures involved. According to Chow,²⁵ factors such as limited access and poor visibility during surgery, flexibility of the long twist drills used in ZI osteotomies, and curved or irregular bony surfaces at the base of the zygoma bone around the exit area can directly affect the level of control over the exit point of the implant.

Important factors to be considered regarding ZI guided surgery are the inherent flexibility of the resin guide, the length of the bur, the angle presented by the outer surface of the maxillary bone, and the lack of a secondary, more apical sleeve along the tubes of the guide to provide supplementary guidance to the crestal metal sleeve. Because the ZI implant positioning is in contact with the external sinus wall, the placement of a second sleeve close to the malar bone was impossible due to the lack of space. Thus, a separate splint was designed for only the 2.35-mm drill (guide A), which has a narrower diameter than the 4-mm-diameter implant. The difference between the two diameters offered the space to form a customized tube only for the 2.35 mm drill along all the external sinus wall. Guide B only provided guidance from the crestal metal sleeve, in addition to the intraosseous pathway that was already prepared using the first drill A more accurate drilling protocol was achieved by avoiding the use of a customized splint for each drill diameter.

Table 2 Outcome Measurements

Implant position		16	13	23	26	Mean	SD
Case 1							
AID		1.38	2.22	1.15	1.8	1.6	0.47
PHD	BP	0.33	0.96	0.13	0.25	0.41	0.37
	MD	0.53	1.3	0.8	1.28	0.97	0.37
AHD	BP	1.05	0.36	0.26	0.36	0.5	0.36
	MD	1.92	2.72	1.7	0.1	1.61	1.09
IDD		0.31	0.7	0.76	1.81	0.89	0.64
IED		0.19	1.31	0.8	1.18	0.87	0.5
Case 2							
AID		0.33	0.86	0.37	0.46	0.5	0.24
PHD	BP	0.27	0.71	0.7	0.16	0.46	0.28
	MD	0.77	0.22	0.95	0.61	0.63	0.31
AHD	BP	0.32	0.24	0.15	0.27	0.24	0.07
	MD	0.38	1.15	0.42	0.71	0.66	0.35
IDD		0.54	0.79	0.22	0.14	0.42	0.3
IED		0.87	0.57	0.72	0.37	0.63	0.21
Case 3							
AID		0.29	0.34	0.94	0.98	0.63	0.37
PHD	BP	1.08	0.77	1.14	0.48	0.86	0.3
	MD	0.96	0.15	0.24	1.43	0.69	0.6
AHD	BP	0.99	0.66	0.27	0.36	0.57	0.32
	MD	0.95	0.71	0.96	2.25	1.21	0.69
IDD		0.3	0.48	0.2	0.71	0.42	0.22
IED		1.05	0.95	1.2	1.79	1.24	0.37
Case 4							
AID		0.34	0.11	0.1	0.76	0.52	0.36
PHD	BP	0.3	0.88	0.63	0.4	0.55	0.23
	MD	0.78	0.55	0.94	0.67	0.73	0.14
AHD	BP	0.23	0.16	0.22	0.57	0.3	0.18
	MD	0.62	0.18	0.2	1.52	0.63	0.63
IDD		0.35	0.36	0.9	0.29	0.47	0.28
IED		0.72	0.39	0.39	1.31	0.7	0.43
Case 5							
AID		0.1	0.65	0.32	1.9	0.74	0.8
PHD	BP	0.78	1.87	0.61	0.13	0.85	0.73
	MD	0.28	0.38	0.9	2.07	0.91	0.82
AHD	BP	0.98	0.33	0.28	0.52	0.53	0.32
	MD	0.4	0.73	0.92	2.79	1.21	1.07
IDD		0.4	0.4	0.97	0.51	0.57	0.27
IED		0.95	0.54	0.59	2.75	1.2	1.04

SD: standard deviation; AID: angular implant deviation; PHD: platform horizontal deviation; AHD: apical horizontal deviation; IDD: implant depth deviation; IED: implant entry point deviation; BP: buccopalatal; MD: mesiodistal. All measurements are in mm except for AID, which are in degrees.

Those four variables—flexibility of the resin guide, length of the bur, angulation of the lateral wall of the maxillary sinus, and extension the drill guidance—may potentially result in variations in the path of the planned ZI position. In view of the above, the bone-supported guide needs to be fixed with two premaxillary fixation pins: one in the malar bone of each maxillary quadrant. Of note was the fact that the whole drilling sequence and placement of the implant was fully guided, because all the steps of the procedure were done through the sleeves of the guides and no margin of maneuverability was allowed by the guides in the current study compared to those used other studies, such as those introduced by Grecchi et al.¹³

CONCLUSIONS

Although the results of the current study are not statistically significant and more cases are needed, the data are encouraging and show substantial accuracy of the procedure, which may improve ZI bone anchorage compared to freehanded implant placement. In-house 3D printers are now a reality due to advances in 3D printing and lowering of the cost of this technology. The customized surgery era is now a reality, being feasible, reliable, and inexpensive when compared to the situation found in the not-too-distant past.

ACKNOWLEDGMENTS

The authors do not have any financial interests, either directly or indirectly, in the products or information listed in the paper.

REFERENCES

- Cawood JI, Howell RA. A classification of the edentulous jaws. *Int J Oral Maxillofac Surg* 1988;17:232–236.
- Rodríguez X, Lucas-Taulé E, Elnayef B, et al. Anatomical and radiological approach to pterygoid implants: A cross-sectional study of 202 cone beam computed tomography examinations. *Int J Oral Maxillofac Surg* 2016;45:636–640.
- Peñarrocha M, Viña JA, Carrillo C, Peñarrocha D, Peñarrocha M. Rehabilitation of reabsorbed maxillae with implants in buttresses in patients with combination syndrome. *J Oral Maxillofac Surg* 2012;70:322–330.
- Peñarrocha M, Carrillo C, Boronat A, Peñarrocha M. Maximum use of the anterior maxillary buttress in severe maxillary atrophy with tilted, palatally positioned implants: A preliminary study. *Int J Oral Maxillofac Implants* 2010;25:813–820.
- Chrcanovic BR, Albrektsson T, Wennerberg A. Survival and complications of zygomatic implants: An updated systematic review. *J Oral Maxillofac Surg* 2016;74:1949–1964.
- Poeschl PW, Schmidt N, Guevara-Rojas G, et al. Comparison of cone-beam and conventional multislice computed tomography for image-guided dental implant planning. *Clin Oral Investig* 2013;17:317–324.
- de Almeida EO, Pellizzer EP, Goiatto MC, et al. Computer-guided surgery in implantology: Review of basic concepts. *J Craniofac Surg* 2010;21:1917–1921.
- D'haese J, Ackhurst J, Wismeijer D, De Bruyn H, Tahmaseb A. Current state of the art of computer-guided implant surgery. *Periodontol* 2000 2017;73:121–133.
- Colombo M, Mangano C, Mijiritsky E, Krebs M, Hauschild U, Fortin T. Clinical applications and effectiveness of guided implant surgery: A critical review based on randomized controlled trials. *BMC Oral Health* 2017;17:1–9.
- Bover-Ramos F, Viña-Almunia J, Cervera-Ballester J, Peñarrocha-Diogo M, García-Mira B. Accuracy of implant placement with computer-guided surgery: A systematic review and meta-analysis comparing cadaver, clinical, and in vitro studies. *Int J Oral Maxillofac Implants* 2018;33:101–115.
- Wu Y, Wang F. Guided and navigation techniques for zygomatic implants. *Atlas Oral Maxillofac Surg Clin North Am* 2021;292:253–269.
- Hung KF, Wang F, Wang HW, Zhou WJ, Huang W, Wu YQ. Accuracy of a real-time surgical navigation system for the placement of quad zygomatic implants in the severe atrophic maxilla: A pilot clinical study. *Clin Implant Dent Relat Res* 2017;19:458–465.
- Grecchi F, Stefanelli LV, Grivetto F, et al. A novel guided zygomatic and pterygoid implant surgery system: A human cadaver study on accuracy. *Int J Environ Res Public Health* 2021;18:6142.
- Landes CA, Paffrath C, Koehler C, et al. Zygoma implants for midfacial prosthetic rehabilitation using telescopes: 9-year follow-up. *Int J Prosthodont* 2009;22:20–32.
- Kreissl ME, Heydecke G, Metzger MC, Schoen R. Zygoma implant-supported prosthetic rehabilitation after partial maxillectomy using surgical navigation: A clinical report. *J Prosthet Dent* 2007;97:121–128.
- Rinaldi M, Ganz SD. Computer-guided approach for placement of zygomatic implants: Novel protocol and surgical guide. *Compend Contin Educ Dent* 2019;40:1–4.
- Rigo L, Tollardo J, Giammarinaro E, Covani U, Caso G. Fully guided zygomatic implant surgery. *J Craniofac Surg* 2021;32:2867–2872.
- Chrcanovic BR, Oliveira DR, Custódio AL. Accuracy evaluation of computed tomography-derived stereolithographic surgical guides in zygomatic implant placement in human cadavers. *J Oral Implantol* 2010;36:345–355.
- Schiroli G, Angiero F, Zangerl A, Benedicenti S, Ferrante F, Widmann G. Accuracy of a flapless protocol for computer-guided zygomatic implant placement in human cadavers: Expectations and reality. *Int J Med Robot* 2016;12:102–108.
- Duarte L, Peredo L, Nary Filho H, Fran-Cischone C, Brånemark P. Rehabilitação da máxima atrófica utilizando quatro fixações zigomáticas em sistema de carga imediata. *Implant News* 2004;1:45–50.
- Migliorança R, Ilg JP, Serrano AS, Souza RP, Zamperlini MS. Sinus exteriorization of the zygoma fixtures: A new surgical protocol. *Implant News* 2006;3:30–35.
- Hernández-Alfaro F, Ragucci GM, Valls-Ontañón A, Hamawandi AA, Bertos-Quílez J. Extramaxillary zygomatic implant coverage with a pedicled buccal fat pad flap through a tunnel approach: A prospective case series. *Int J Oral Maxillofac Implants* 2022;37:400–406.
- Bertos Quílez J, Guijarro-Martínez R, Aboul-Hosn Centenero S, Hernández-Alfaro F. Virtual quad zygoma implant placement using cone beam computed tomography: Sufficiency of malar bone volume, intraosseous implant length, and relationship to the sinus according to the degree of alveolar bone atrophy. *Int J Oral Maxillofac Surg* 2018;47:252–261.
- Bover-Ramos F, Viña-Almunia J, Cervera-Ballester J, Peñarrocha-Diogo M, García-Mira B. Accuracy of implant placement with computer-guided surgery: A systematic review and meta-analysis comparing cadaver, clinical, and in vitro studies. *Int J Oral Maxillofac Implants* 2018;33:101–115.
- Chow J. A novel device for template-guided surgery of the zygomatic implants. *Int J Oral Maxillofac Surg* 2016;45:1253–1255.